ECE 445: Final Report

Microphone Probe for Measurement of

Specific Acoustic Impedance of Ground

Team #48: Anna Czerepak, Kevin Looby

May 2, 2013

Abstract

Our senior design project was done in collaboration with Dr. G. Swenson and Dr. M. White at the Construction Engineering Research Laboratory in Champaign, Illinois. The aim of our project was to develop an improved version of the hardware they previously used to measure the specific acoustic impedance of ground *in-situ*. The results of their measurements did not fit to any parameters tried in their model and broke down below frequencies of 50 Hz. By redesigning the microphones used, building our own probe housing and stake, designing our own preamplifiers, and testing the output of the loudspeaker used in the tests, our group hopes to provide our collaborators with hardware that is designed specifically to be used to measure to frequencies from 10 Hz up to 1 kHz. By doing this, we aim to eliminate as much potential error as possible from defects in design or selection of the hardware and help them improve the results of their measurements of specific acoustic impedance of surfaces.

Contents

1 Introduction

1.1 Purpose and Function of Project

Researchers at CERL (the Construction Engineering Research Laboratory) in Champaign, Illinois have made attempts to obtain measurements of the acoustic impedances of surfaces and materials. Their previous experimental setup required immense computation power and did not provide conclusive results. The purpose of this project is to design and implement a more elegant hardware setup to be used in the determination of the specific acoustic impedances of surfaces, especially that of the ground. The function of our system will take measurements of acoustic pressures using an array of four pressure microphones. The data collected by this system will then be amplified and sent out to a collection unit to be saved and manipulated. In this way, we hope to produce hardware that is reliable and verified to be free from instrumentation or design errors so that the data that is acquired will be easier to use to determine the specific acoustic impedance of the surface being measured.

1.2 Modules

A block diagram of the project modules is presented in Figure 1.

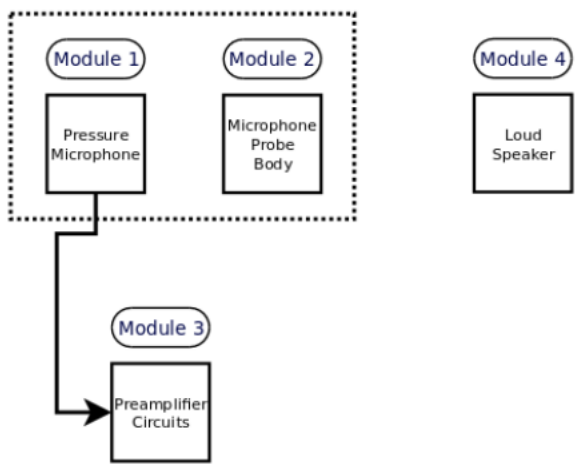

Figure 1: Block diagram of the project modules.

The detailed descriptions of each module and the connections between modules is found in Section 2.

2 Design

2.1 Module 1: Microphones

2.1.1 Design Procedure

The microphones formed the centerpiece of our probe and thus needed to be selected carefully. The microphones needed to be sensitive (especially to low frequencies such as those under 100 Hz) in order to pick up the small variations in the pressure field being measured. They needed to be small in order to not interfere with the acoustic waves incident on and reflected from the ground being measured. The microphones needed to be omni-directional in order for the measurement technique used to be applied (the “p-p method”). They needed to be able to be affixed to the rest of the probe components in a stable manner so that they do not shift during transport and measurement. Additionally, any wires coming from the microphones needed to be small in gauge and be located so that they may be soldered to without placing any mechanical stress on the solder pads. The last requirement was to find microphones that required a voltage that could be supplied off of the same +15 V/-15 V power supply that the preamplifier circuits require.

2.1.2 Design Details

The microphones picked for this module were four electret condenser-type Knowles Electronics omni-directional pressure microphones, model number WP-23502. This particular series of Knowles Electronics microphones are water-proof and miniature. The concern with most traditional electret microphones is the vent hole that is usually made in the diaphragm of the microphones. The vent hole helps to equalize the pressure behind the microphone (which is an otherwise closed cavity) so the diaphragms do not blow out. The response to high frequency acoustic inputs is not compromised by the diaphragm hole, however it interferes significantly with the microphone response at low frequencies. Because the WP-23502 model is water-proof, it does not have the diaphragm hole and its low frequency sensitivity is not compromised.

The WP-23502 models are very small and delicate, giving rise to the need to affix them to some backing for stability and ease of manipulation. To accomplish this, the microphones were glued (with 'Locite' brand cyanoacrylate glue) to the aluminum microphone cap (a part of the microphone probe body assembly). It also ensures the the three wires soldered to the output pads of the microphones do not touch or break because of mechanical stresses.

The three output wires from each microphone were designed to go through a drilled hole in the microphone cap, through the hollow wand, and soldered to the input pins on the preamplifier circuit. The pressure microphones nominally require +1.3V across the positive and negative terminals to function, which is sufficiently small enough to be supplied by the preamplifier circuit. Our preamplifier supplies +1.8V to each microphone. Since the microphones are specified to be functional up to +10V DC voltage, this is an acceptable supply voltage.

2.2 Module 2: Microphone Probe Body and Stake

2.2.1 Design Procedure

The probe housing module would house the microphones and the preamplifiers, it needed to also be stable in order to resist vibrations that could be induced by the acoustic waves provided by the loudspeaker source. The entire design needed to be modular, so that components could be re-machined if needed and able to be disassembled for storage and transport. This module also needed to be light so that it is not difficult to transport to the measure site. The individual pieces of this module needed to connect to each other securely so that the instrument is stable and does not break the electrical connections or cause any part to become loose when measurements are being preformed. This module also needs to maintain the four microphone probes at a stable and fixed distance from each other. This is because the p-p method for measuring particle velocity (and by extension, specific acoustic impedance) relies on approximating a pressure gradient as the difference in pressures divided by the distance [2]. This approximation makes the p-p method very sensitive to the microphone spacing. The errors inherent in the finite difference approximation can be seen in Appendix A. The final requirement was that the microphones somehow be put far enough away from the rest of the module to minimize diffractive interference off of the probe housing.

2.2.2 Design Details

The final probe body design consists of two main parts; the microphone probe housing and the stake. An image of the entire module assembled is shown in Figure 2.

Figure 2: The microphone probe array assembled.

Microphone Probe Housing

The purpose of the microphone probe housing is to house the microphones and the preamplifier circuits. An image of the completed microphone probe housing assembled and disassembled in shown in Figure 3.

Figure 3: (Top) A single microphone probe body assembled. (Bottom) A disassembled microphone probe body.

The probe housing consists of four separate pieces; the microphone cap, the wand, the preamplifier housing, and the connector converter. Its function is to house each microphone and its preamplifier circuit and hold each microphone in a fixed location. Additionally, though it was not done in the scope of this project, it could provide additional shielding for the signals from microphone if conducting lug nuts were drilled into each piece and connected to a common ground.

Each piece of the microphone housing was constructed out of a solid, continuous piece of stock 6061 aluminum alloy. Aluminum was selected because of its light weight, bending resistance to modest stresses, and ease of machinability.

Threaded connections were the first choice for stability and disassembly. However, threaded connections could not be used for certain connections to avoid twisting electrical wires. To avoid this problem, set-screws were used in these instances to hold the parts together.

The microphone cap diameter matches the outside diameter of the wand, making a smooth, continuous fit between the cap and wand that does not introduce unwanted acoustic reflections. The base of the microphone cap has an outer diameter that matches the inside diameter of the bore hole through the wand. The microphone cap has a small, recessed slot that ensures uniform positioning of the microphones. A small, counter-sunk hole drilled through the cap allows the wires to pass through the bottom of the cap to the wand.

The primary purpose of the wand is to distance the microphones from the bulkier preamplifier housing and stake to minimize acoustic diffraction. To accomplish this, we chose a length of 8". The preamplifier housing attaches at the opposite side of the wand via a tapped hole that matches with the outside thread size on the last 1" of the microphone wand.

The preamplifier housing contains the preamplifier circuits, which amplify the small voltage output of the microphone and supply power to each microphone. The circuits are shielded from the conductive housing by a Teflon tube.

The type of connector we wanted to use between the microphone probes and the stake was a challenge to pick. The connection needed to bear the weight of the entire microphone probe housing, as well as the microphones and preamplifier circuits. This made most common electrical connectors (such as BNC connectors and banana plugs) unsuitable. After much searching, a four-pin thread-locking microphone connector was chosen. However, the microphone connector had an outer diameter of 5/8" and the inner diameter of the preamplifier was 3/4". To join these two pieces in a satisfactory way, the connector converter cap was necessitated. The connector converter screws onto the the preamplifier housing via an external threaded section. It has an inner diameter hole that matches the outer diameter of the male four-pin microphone connector. The connector is attached to the connector converter via four set-screws which fit into holes drilled 90 degrees apart on the outside of the connector converter. Under normal assembly, the connector is left free until the converter is screwed onto the preamplifier housing. The converter is then gently pushed into the connector converter and the four set screws are screwed into place.

Stake

The second component of the microphone probe housing is the stake. The purpose of the stake is to provide a secure anchor point for the microphone probes and to provide a connection between the power supply and output of the preamplifiers. An image of the completed stake is shown in Figure 4.

The stake is made out of a 15" long 6061 aluminum alloy, rectangular tubing. On the front face, it has four equally-spaced (10 cm center-to-center) holes that provide a place to secure the microphone connectors. On the back side, are larger-diameter clearance holes that allow the cable connections to be manipulated and each lock-washer to be tightened. The bottom of the back face has holes for four BNC female cables. Above this are three, chassis-mount plastic banana jacks for the power supply cables.

Inside the stake, the signal from each microphone probe goes through a male and female microphone connector, down a shielded BNC cable, and out to the data collection unit through the the female-ended BNC near the bottom. Each microphone power pin is connected to the banana jack on the stake by a 20 AWG, solid-core hookup wire.

2.3 Module 3: Preamplifier Circuits

Each of the four microphones used in our system requires a dedicated preamplifier circuit. In choosing a design for the preamplifier, it was important to take into consideration noise production, cost, sensitivity, and gain. Additionally, a very compact design was needed, as these preamplifiers are housed in the probe bodies. The casing was designed to be as minimal as possible in order to minimize interference effects.

2.3.1 Design Procedure

The general preamplifier circuit design used with the selected microphones was provided by Professor Steve Errede [4], who has extensively made use of microphones similar to those selected for this project. Minor modifications have been made to his original design in order to obtain a more linear response for the lower

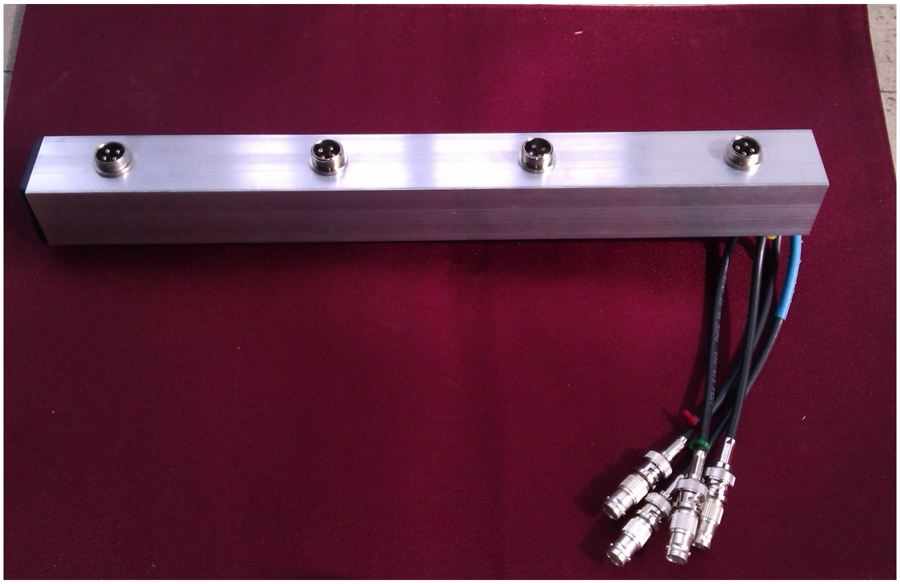

Figure 4: The front of the stake, showing male microphone connectors and BNC output cables.

acoustic frequencies important to this project. A schematic of the circuit can be found in Appendix B, along with the microphone equivalent circuit used for simulation purposes.

The circuit components selected were chosen in order to reduce potential noise sources as much as possible. Only metal film resistors were used so that contact noise could be reduced, and the LF411CP operational amplifier used in these circuits advertises a very low noise floor.

2.3.2 Design Details

The preamplifier circuit was simulated using National Instruments Multisim in order to calculate the ideal gain to be expected of the circuit and evaluate the response of the circuit over the range of frequencies most important to our application (frequencies less than 1000 Hz). The AC analysis performed in Multisim is provided below in Figure 5. Both the magnitude and phase responses are constant in the frequency range of most interest. Because the phase response of the circuit is non-ideal at very low frequencies, the response of each preamplifier has been characterized. Information regarding the individual phase responses of each constructed preamplifier circuit is presented in Section 3.

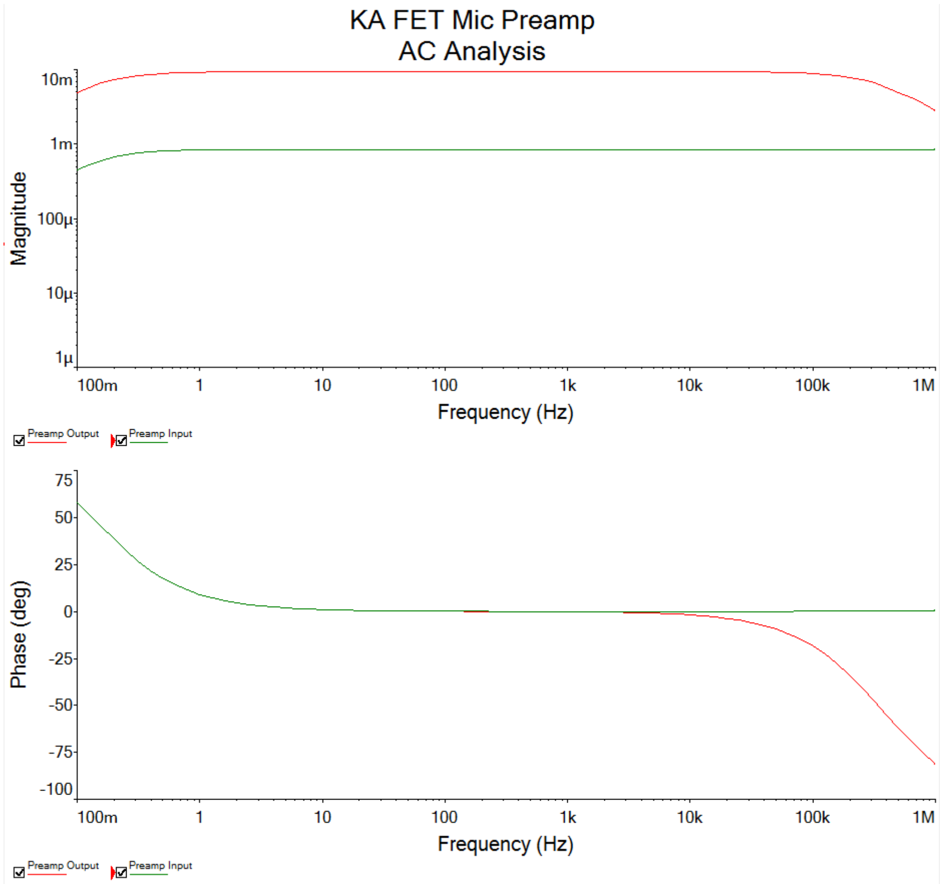

Figure 5: AC analysis for simulated preamplifier circuit

Data from the AC analysis was exported to Wolfram Mathematica for further manipulation. The simulated output of the preamplifier was divided by the input curve in order to produce the gain curve provided in Figure 6. The data was further analyzed in order to calculate the -3 dB cutoff of the preamplifier. This cutoff was found to be at approximately 316 kHz, which is well outside the range of frequencies that will be looked at by our system. This, along with the results of the AC analysis, clear this circuit as a very good choice for low-frequency signals.

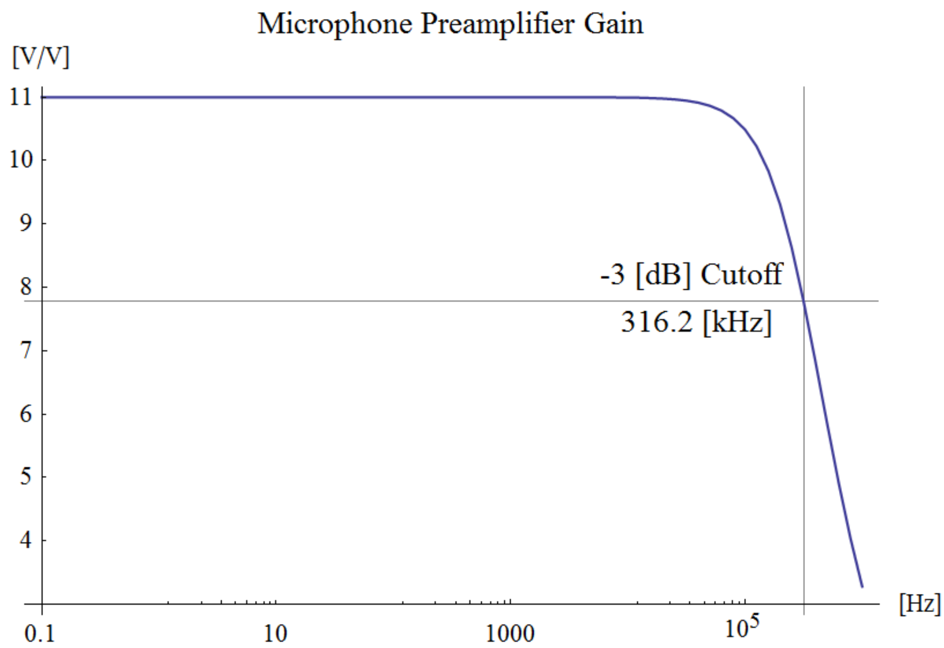

Figure 6: Simulated gain as a function of frequency for microphone preamplifier circuit.

3 Requirements and Verifications

The requirements, verifications, and results of each module are presented in table form in Appendix E.

3.1 Module 1: Microphones

3.1.1 Microphone Sensitivity

The most important consideration in acquiring reliable and precise measurements with the p-p method is the absolute pressure calibration and measurement of the frequency response and phase response of each microphone-preamplifier pair. The p-p method relies on each microphone in the array having the same frequency and phase responses. However, because each microphone has slightly different response curves due to variances in manufacturing, there is no guarantee that the frequency and phase responses of each of our four microphones are exactly the same. If these two curves are known for each microphone-preamplifier pair, the data from each pair can be corrected in the analysis phase of the experiment, after the measurements are made.

The requirements that needed to be met for the microphones, once a suitable model was chosen, were minimal. Though the microphones are arguably the most important part of the microphone probe project, there were no design decisions that went into each microphone once they were purchased. Some of the tests that our group would have like to have preformed were unfortunately beyond the facilities and equipment available to us. One example of this would be a test of the actual polar plot directionality of the microphones to confirm that the microphones purchased were omni-directional. This would have required an acoustic anechoic chamber and several measurement microphones. Everitt Laboratory has a radio frequency anechoic chamber, but after discussion with professors that manage the chamber, it was deemed to be not a close enough approximation to an acoustic anechoic chamber to be worth doing the test.

The one requirement that our group did insist on and test was the sensitivity of the microphone. The magnitudes of the pressure field above the ground surface for the acoustic impedance measurements could be very small, and it was imperative that the microphones we used have a high sensitivity at low acoustic pressures. The requirement was a voltage output sensitivity of -50 dB ($\pm$3 dB) at an SPL (sound pressure level) of 94 dB (relative relative to reference pressure $p_0 = 2 \cdot 10^{-5}$ Pa, corresponding to an SPL of 74 dB). To accomplish this, it was necessary to measure the voltage output of a microphone when it is immersed in a field with local SPL=74 dB and SPL=94dB with a digital multimeter. The microphones were fixed into a holder one meter away from a horn loudspeaker. The horn loudspeaker was turned on and the volume adjusted until the local sound pressure at the microphone was the correct value. The voltage output was then read from the attached multimeter and recorded. The calculation used to determine the sensitivity from this data is given below:

$$SPL\,(dB) = p\,(dB) = 20 \cdot \log\left[\frac{p}{p_0}\right] \tag{1}$$

$$p\,(Pa) = p_0\left(\exp\left[\frac{SPL\,(dB)}{20}\right]\right) \tag{2}$$

$$S_{p-mic}(V/Pa) = \frac{V_{p-mic}}{p} \tag{3}$$

$$S_{p-mic}(dB) = 20 \cdot \log\left[\frac{S_{p-mic}}{S_{0-p-mic}}\right] \tag{4}$$

This requirement was verified and successfully passed. The measured voltage outputs were $V_{p-mic-1} = 8.02$ mV at SPL=74 dB and $V_{p-mic-2} = 809.6$ mV at SPL=94dB. This gives us a sensitivity of $S_{p-mic} = -50.1$ dB, which is within the requirement range.

3.2 Module 2: Microphone Probe Body and Stake

3.2.1 Vibration Stability

The method to verify that the design of the microphone probe housing would not vibrate under normal measurement conditions was to preform a COMSOL simulation of the entire probe. This could be used to obtain the eigenfrequencies and eigenmodes of the structure. This yields information about the way that the probe housing vibrates and at what frequencies the vibrations are maximally excited.

Our plan was to check that the lowest eigenfrequency is above the upper-limit of the frequency range measured (about 1kHz). The CAD models of each microphone probe component were made in the CAD program SolidWorks and imported into COMSOL. A simple eigenfrequency study was run with a very fine mesh sizing (about 1 cm^2 per mesh) but the results of the simulation showed that the lowest eigenfrequency obtained was 31324 Hz. Dividing this frequency by 6240 m/s, the speed of sound in aluminum, it was found that the wavelength corresponding to this eigenmode would be 5.0198 m. This is nowhere near the approximate expected wavelength of the lowest mode (which should be about equal to half the length of the stake, or 19 cm) and thus indicates that the simulation was not preformed accurately.

However, given that the power incident on the probe from the SuperCube II loudspeaker is over 2 meters away and is limited by the maximum power output of the loudspeaker (and the fact that power at a distance r from the source decreases with $\frac{1}{r^2}$), the vibrations from incident sound should not be a problem. Nevertheless, the vibration stability requirement was not met because the test was not preformed reliably.

3.2.2 Acoustic Diffraction

The probe body was supposed to be designed to minimize acoustic diffraction at frequencies under 1 kHz. To do this, two COMSOL simulations were planned. One simulation would place the CAD model of the microphone probe near a flat surface to simulate testing conditions. An acoustic dipole source would be placed directly above the plane of the microphones and the pressure field around the probe would be analyzed. The same setup without the microphone probe (with just the flat surface and the acoustic dipole source) would be run and the pressure field at 300 evenly-distributed points would be sampled from each simulation result. The difference in pressure fields at each point could be calculated and a percentage difference obtained. The requirement was that the percent difference at each point be no more than $10\% \pm 5\%$.

However, this test could not be preformed at this time. The CAD models were loaded into COMSOL and the surface and microphone probe placed. The acoustic source could not be simulated and that was why this test was not done. The only acoustic sources that were available in the Acoustics Module of COMSOL 4.3

were infinite plane wave sources. This would not accurately model the shape of the acoustic waves produced by the loudspeaker during measurements. Because of this, the acoustic diffraction simulation was not useful for testing the acoustic interference caused by the microphone probe.

The probe body module did not pass the acoustic diffraction requirement as the test could not be preformed reliably. The simulation will be retried again in the future, as it could reveal points that the probe housing diffracts a significant amount of incident acoustic waves into. If one of these points were to be a midpoint between two of the microphones, this would give artificially high values for the pressure gradient above the surface. However, higher-frequency waves are more prone to scattering. Because the highest acoustic frequency tested was 1kHz and lower-frequency waves do not diffract significantly off of objects smaller than their wavelength, it is not likely to suspect that any sort of significant diffraction is taking place during measurement.

3.3 Module 3: Preamplifier Circuits

3.3.1 Voltage and Current Delivered to Microphone

We required that the voltage delivered to each microphone by the preamplifier circuit be between 1 V and 2.5 V in order to assure proper function. Before installing the microphones, a resistor of equivalent resistance (22 kΩ) was inserted into the circuit in place of the microphone in order to test the expected voltages and currents that would be applied to the microphone. For reference, the microphones have a resistance of approximately 23.0 kΩ across the power supply terminals. Table 1 summarizes the voltages and currents measured across the 22 kΩ resistor.

Table 1: Measured voltages and currents across microphone-equivalent resistor.

Preamplifier Circuit	**Measured Voltage [V]**	**Measured Current [mA]**
#1	1.220	0.635
#2	1.670	0.646
#3	1.645	0.622
#4	1.533	0.640

All of these measured voltages and currents are well within the tolerances of the microphones, clearing all four constructed preamplifier circuits as safe for use with the microphones.

3.3.2 Gain

Each preamplifier was designed to provide an ideal gain of 11 V/V. For the purposes of this project, the acceptable tolerance set for the gains of the preamplifiers was 11 ± 3% V/V with a flat frequency response over the range 1 Hz to 1 kHz. This strict restriction on the tolerance was required in order to ensure that the signal amplitudes output by each preamplifier accurately reflect the relative amplitudes of the signals measured by the microphones. Figure 7 shows the the calculated gain as a function of frequency for each of the four preamplifiers, plotted alongside the ideal simulated gain.

The data for these plots was taken by performing an electrical AC sweep before the microphones were connected to the circuit. A National Instruments myDAQ and National Instruments Elvismx software were used to perform an AC sweep from 1 Hz to 1 kHz. The myDAQ's ±15 DC power supply lines were used to power the preamplifier circuit, and its analog output channel was used to deliver the test signal to the terminal that would later be connected to the microphone output. The myDAQ has two channels for measuring analog inputs. One channel was used to measure the signal entering the preamp circuit, and the other measured the signal output by the preamp.

National Instruments Elvismx software contains a function generator to be used with the NI myDAQ. This function generator was configured to perform an AC sweep from 1.0 Hz to 1.0 kHz increasing in intervals of 1 Hz. Each discrete frequency was held for a duration of 1000 ms (1.000 s). The peak-to- peak amplitude of the test signal for these sweeps was 0.1 V. Preliminary testing of the microphones showed that typical output voltages range from 0.03 V to 0.15 V. The voltage of 0.1 V was selected for the AC sweeps as it was representative of typical voltages to be expected from the microphones.

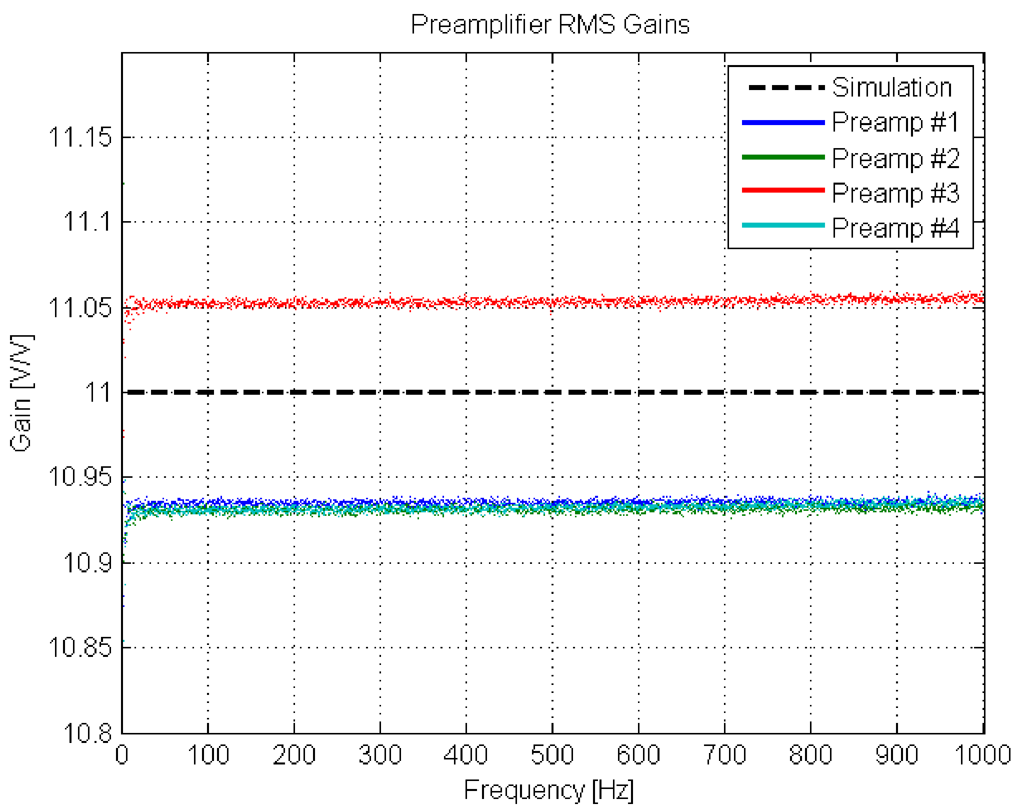

Figure 7: Calculated RMS gains for preamplifier circuits with model.

MATLAB was used to read in and store the data measured by the myDAQ (see Appendix D for the MATLAB code used). After the AC sweeps had been performed for each of the preamplifiers, the RMS gains were calculated using MATLAB. Before further manipulation, the DC offset of the output signals (about 1.3 V, with slight variations between each preamp) was removed by subtracting the mean of the signal from each data point. The gain plots shown in Figure 7 were then calculated using a windowed RMS method. The sampling rate used to measure the data was 2 kHz, and each frequency was held for a duration of 1 s. Thus, each discrete frequency in the sweep was represented by 2000 data points. Matlab was then used to calculate the RMS amplitude in windows of 2000 data points for both the input signals and the output signals. The calculated RMS amplitudes of the output signals were then divided by the RMS amplitudes of the input signals, providing the data plotted in Figure 7.

The following data in Table 2 presents the mean values and standard deviations for the calculated gains for each of the preamplifier circuits. As mentioned previously, the required tolerance set for the gains was 11 ± 3% V/V, which restricts the gains to be within the range [10.67, 11.33] V/V. The calculated values presented below are well within these tolerances. Additionally, it is not a significant problem that the mean gain of preamplifier #3 varies from the mean gains of the other preamplifiers. However, this difference must be documented so that it can be accounted for when interpreting data collected by this instrument.

Table 2: Measured mean gain and gain standard deviations.

Preamplifier	**Mean Gain [V/V]**	**Standard Deviation [V/V]**
#1	10.9350	0.0089
#2	10.9311	0.0074
#3	11.0527	0.0384
#4	10.9325	0.0193

3.3.3 Phase Response

The phase delay between the input and output of the preamplifier circuits was an important consideration in the design and characterization of the preamplifiers. The circuit, as designed, has a moderate phase delay for very low frequencies. This low-frequency delay comes primarily from the blocking capacitor at the output of the microphone and its effects can ideally be considered negligible above roughly 20 Hz. However, as this project seeks to function at infrasonic frequencies, the phase responses of each of the preamplifier circuits were characterized so that delays could be taken into consideration when performing calculations on data collected by this system.

Phase delays were measured using an Agilent Technologies InfiniiVision DSO714B oscilloscope. Similar to the experimental setup used to measure the gain responses of the preamplifiers, the NI myDAQ was used to power the circuit and feed an input into the preamplifier. The oscilloscope was was set up to monitor both the input and output signals of the preamplifier and configured to calculate the relative phase between the two signals. Pure sinusoidal signals of varying frequency were then generated using the Elvismx function generator, and the relative phases calculated by the oscilloscope were recorded. The results for the four preamplifier circuits are plotted in Figure 8, along with the ideal phase response from the circuit simulation.

Very good agreement was found between the four sets of measurements and the simulated model. The purpose of this test was to characterize the phase responses of each of the preamplifier circuits for future reference and to verify that each behaved as expected, which was accomplished.

3.4 Module 4: Loudspeaker

3.4.1 Output

An additional test was done on the loudspeaker used in the original measurements (made by Jeffrey Borth) in order to check the loudspeaker itself for sources of errors in the data. To do this, we measured and verified the actual lower frequency limit of the loudspeaker output. The results of the output at the four measured lowest frequencies are shown in Figure 9. For reference, the manufacturer-listed frequency range of the SuperCube II is 14-200 Hz.

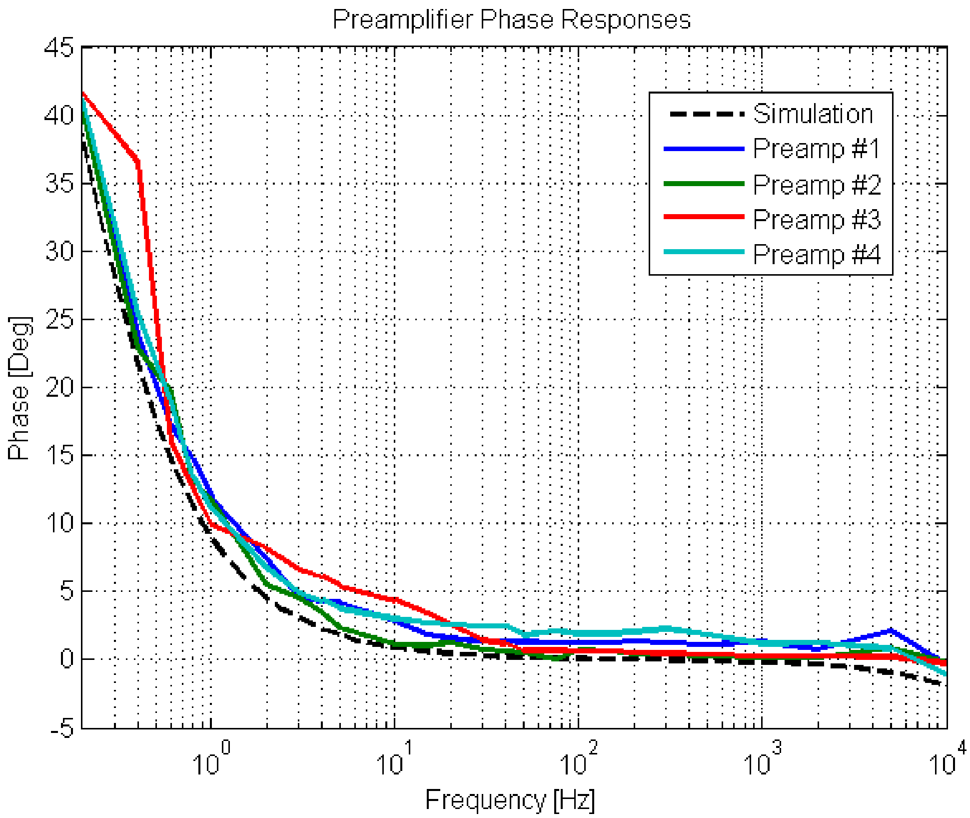

Figure 8: Measured phase responses of preamplifier circuits compared with the model.

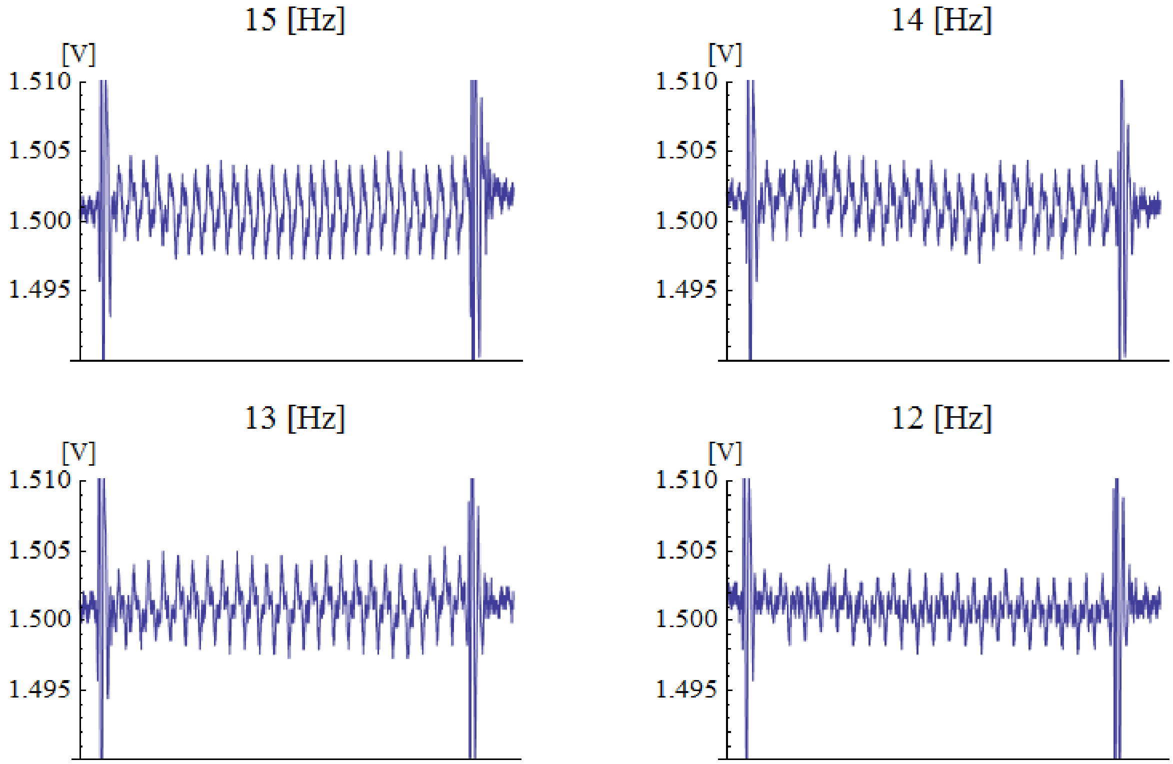

Figure 9: Low-frequency limit measurements of loudspeaker output

These measurements were taken using one of our assembled microphones and preamplifiers. Matlab was then used to generate a pure sinusoidal audio output of controllable frequency that was used to drive the loudspeaker. An oscilloscope was consistently capable of detecting the frequency of the output signal down to 13 Hz, however this required that the microphone be in very close proximity to the loudspeaker and that the amplification on the loudspeaker be near its maximum. The oscilloscope was only sporadically able to identify the 12 Hz signal, and all tested frequencies below 12 Hz were undetectable.

From our experiments we were able to verify that the SuperCube II is capable of producing acoustic waves at the frequencies specified by the manufacturer. However, our measurements were taken in an enclosed space that was relatively isolated from noise. Despite this, detection of the lowest frequencies required close proximity to the loudspeaker and high amplification. The loudspeaker output under measurement conditions could differ significantly and be undetectable by the microphone probe. Further investigations need to be made to determine how far this loudspeaker is able to propagate very low-frequency pressure waves. This is especially important to remeasure in the very non-ideal environment used to test ground impedances, where distance and wind noise may make measurements of this frequencies impossible without further amplification of the acoustic source.

4 Costs

The complete and detailed table of cost of parts (separated by module) is included in Appendix C.

4.1 Parts

Parts costs are calculated as follows:

$$\text{Parts Cost (Total)} = \text{Parts Cost (Module 1)} + \text{Parts Cost (Module 2)} + \text{Parts Cost (Module 3)}$$

$$= \$126.60 + \$111.11 + \$29.51$$

$$= \$267.22$$

4.2 Labor

Labor costs are calculated as follows:

$$\begin{aligned}
\text{Labor Cost (Kevin)} &= \text{Hourly Rate} \times \text{Hours Worked} \times 2.5 \\
&= \frac{\$55}{[\text{hr}]} \times 138\ [\text{hr}] \times 2.5 \\
&= \$18,975.00
\end{aligned}$$

$$\begin{aligned}
\text{Labor Cost (Anna)} &= \text{Hourly Rate} \times \text{Hours Worked} \times 2.5 \\
&= \frac{\$55}{[\text{hr}]} \times 145\ [\text{hr}] \times 2.5 \\
&= \$19,937.50
\end{aligned}$$

Total Labor Cost: **$38,912.50**

4.3 Total Cost

The total cost for this project up to this point is as follows:

$$\begin{aligned}
\text{Total Cost} &= \text{Parts Cost} + \text{Labor Cost} \\
&= \$267.22 + \$38.912.50
\end{aligned}$$

$$= \$39,179.72$$

5 Conclusion & Future Work

At the time of writing, the microphone probe array is functional and fulfills most of the basic requirements our group specified at the beginning of this project. The microphone probe housing, the stake, and all associated cables and connections are constructed and fit together as intended. From coarse-grained physical tests, the entire assembly seems stable against vibrations and maintains a constant spacing between the microphones very well when the threaded microphone connectors and the lock washers are tightened.

Future work will be to calibrate the microphones and to measure and record each microphone's frequency and phase response. Also, the failed COMSOL simulation for the eigenfrequencies of the microphone probe body and the COMSOL simulation for the acoustic diffraction will be reattempted.

A Approximation Errors in p-p Method

One of the largest source of systematic error when using the p-p method stems from the use of finite difference approximations on the pressure and particle velocity.

According to the Taylor series expansion

$$p(x+h,t) = p(x,t) + hp^{'}(x,t) + \left(\frac{h^2}{2}\right)p^{''}(x,t) + \left(\frac{h^3}{6}\right)p^{'''}(x,t) + \ldots + \left(\frac{h^n}{n}\right)p^n(x,t) + \ldots \tag{5}$$

where $p(x,t)$ has arbitrary time dependence and $p^n(x,t)$ denotes the nth derivative of p with respect to x at any instant t. If the pressure difference between two microphones separated by a distance $d = 2h$ is measured, the estimated pressure at a point midway between the two can be written (dropping explicit spatially-dependent terms)

$$p_e(t) = \frac{1}{2}\left[p_2(t) + p_1(t)\right] \approx p(t) + \left(\frac{h^2}{2}\right)p^{''}(t) + \left(\frac{h^4}{24}\right)p^{iv}(t) + \ldots \tag{6}$$

And a estimate of the particle velocity midway between them can be written

$$u_e(t) = -\left(\frac{1}{\rho_0}\right)\int\limits_{-\infty}^{t}\left[p^{'}(\tau) + \left(\frac{h^2}{6}\right)p^{'''}(\tau) + \left(\frac{h^4}{120}\right)p^{iv}(\tau) + \ldots\right]d\tau \tag{7}$$

This gives a normalized errors for pressure $(e(p))$ and particle velocity $(e(u))$ that are equal to

$$e(p) = \frac{(p_e - p)}{p} = \frac{\left[\left(\frac{h^2}{2}\right)p^{''}(t) + \left(\frac{h^4}{24}\right)p^{iv}(t) + \ldots\right]}{p(t)} \tag{8}$$

$$e(u) = \frac{(u_e - u)}{u} = \frac{\int_{-\infty}^{t}\left[\left(\frac{h^2}{6}\right)p^{'''}(\tau) + \left(\frac{h^4}{120}\right)p^{v}(\tau) + \ldots\right]d\tau}{\int_{-\infty}^{t}\left[p^{'}(\tau)\right]d\tau} \tag{9}$$

Since these errors cannot be evaluated unless an explicit form for p and u are provided, two forms used in the original experiment's calculations are considered in Table 3 below; incident and reflected plane waves and spherical waves.

Table 3: A table showing error estimates for two acoustic wave forms.

	Wave Form	Type	Normalized Error Estimate
$e(p)$	$P = A\exp(-ikx) + B\exp(ikx)$	Plane Waves	$\cos(kh) - 1 \approx -\frac{(kh)^2}{2} + \frac{(kh)^4}{24} - \frac{(kh)^6}{720} + \ldots$
	$P(r) = \left(\frac{A}{r}\right)\exp(-ikr)$	Spherical Wave	$-\frac{(kh)^2}{2} + \left(\frac{h}{r}\right)^2 + i(kh)/\left(\frac{h}{r}\right)$ (for $kr \ll 1$)
$e(u)$	$P = A\exp(-ikx) + B\exp(ikx)$	Plane Waves	$\frac{\sin(kh)}{kh} - 1 \approx -\frac{(kh)^2}{6} + \frac{(kh)^4}{120} - \frac{(kh)^6}{5040} + \ldots$
	$P(r) = \left(\frac{A}{r}\right)\exp(-ikr)$	Spherical Wave	$\frac{(kh)^2}{6} + \left(\frac{h}{r}\right)^2$ (for$kr \ll 1$)

B Circuit Schematics

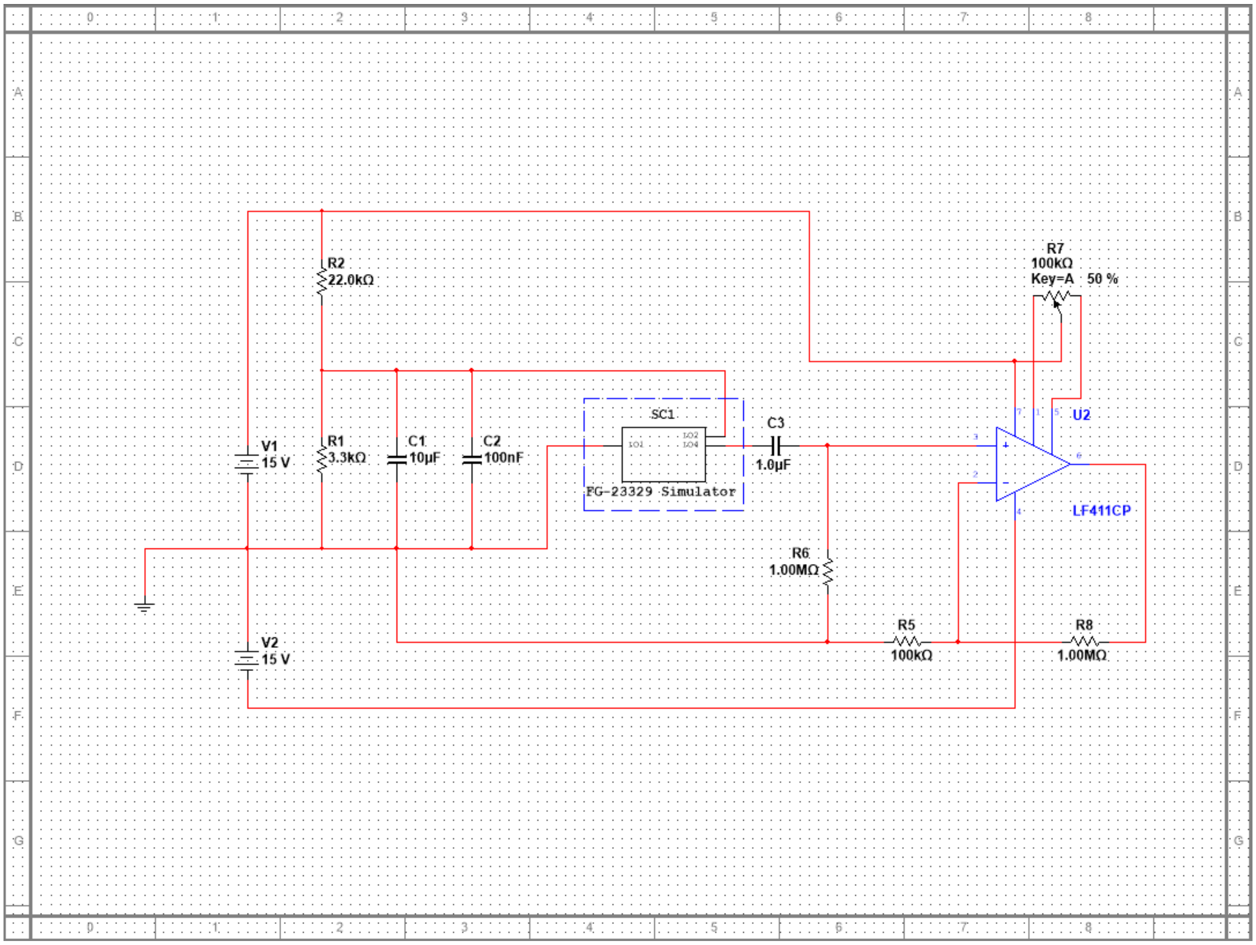

Figure 10: Preamplifier and microphone-powering circuit schematic

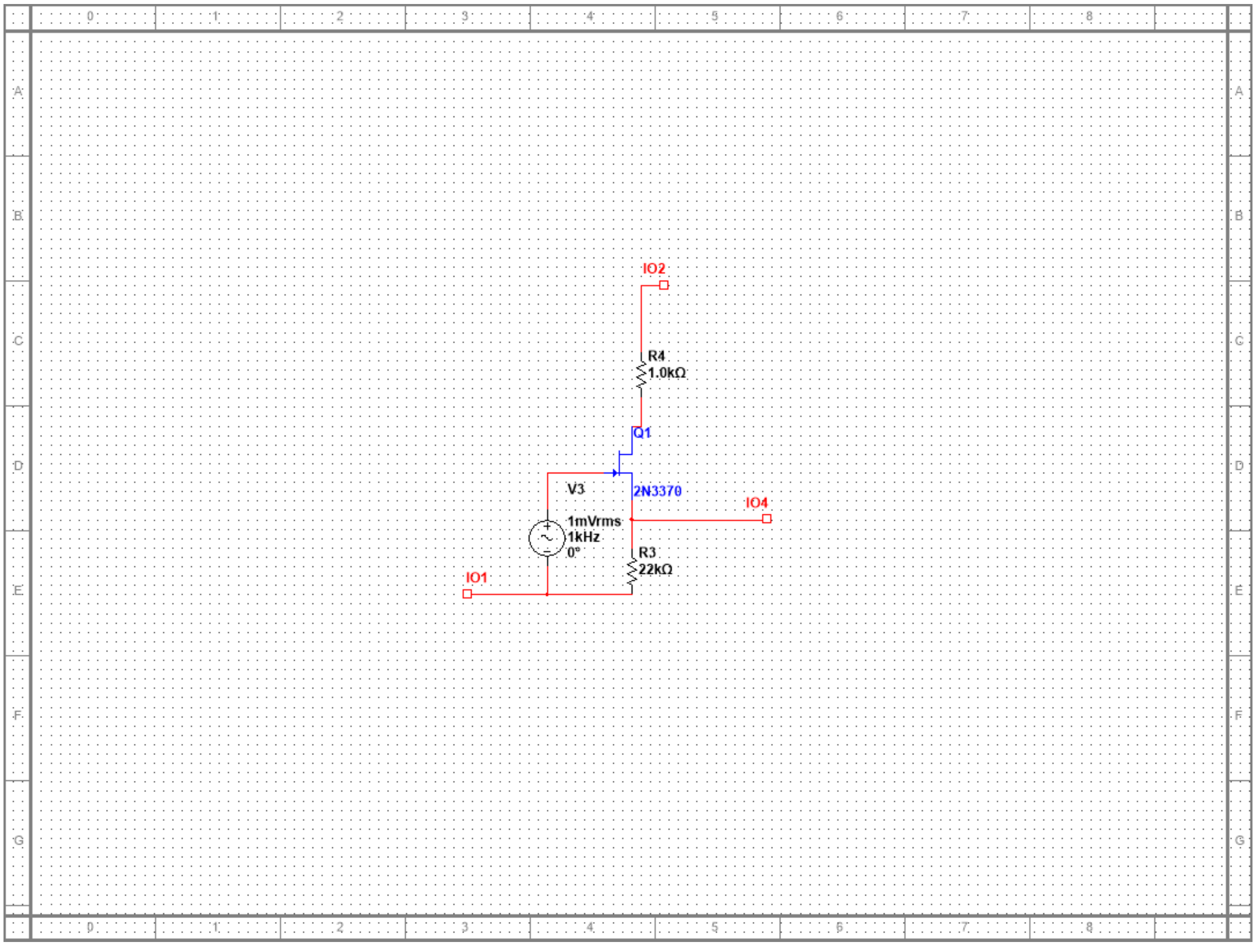

Figure 11: Microphone equivalent circuit for simulations

C Parts Lists

C.1 Microphones

Table 4: The cost of parts table for the microphone module.

Description	Source	Part Number	Unit Price	Quantity	Extended
Knowles Electronics Miniature Microphone (WP-23502)	DigiKey	423-1054-ND	$31.65	4	$126.60
				TOTAL	**$126.60**

C.2 Microphone Probe Housing

Table 5: The cost of parts table for the microphone probe housing module.

Description	Source	Part Number	Unit Price	Quantity	Extended
6061 Aluminum Rect. Tubing (1/8" Wall, 1-1/2" X 1-1/2")	McMaster-Carr	6546K223	$25.32/3' length	3'	$25.32
6061 Aluminum Solid Rod (1" Diameter)	McMaster-Carr	8974K133	$19.34/3' length	3'	$19.34
6061 Aluminum (3/8" Diameter)	McMaster-Carr	8974K32	$11.85/6' length	6'	$11.85
Plastic End Cap for Aluminum Tubing	McMaster-Carr	8809T41	$1.16	1	$1.16
Teflon Tubing (11/16" ID, 3/4" OD, 1/32" Wall)	McMaster-Carr	52355K92	$6.76/1' length	2'	$13.52
4-Pin Microphone Male Connector (Chassis Mount)	Vetco Electronics	CAL-30-454	$4.99	4	$19.96
4-Pin Microphone Female Connector (Inline)	Vetco Electronics	CES-31-1004	$4.99	4	$19.96
				TOTAL	**$111.11**

C.3 Preamplifier Circuits

Table 6: The cost of parts table for the preamplifier module.

Description	**Source**	**Part Number**	**Quantity**	**Unit Price**	**Extended**
Op Amp	DigiKey	LF411CP	4	\$1.71	\$6.84
Metal Film 22kΩ Res.	DigiKey	HHV-25JR-52-22K	4	\$0.31	\$1.24
Metal Film 3.3kΩ Res.	DigiKey	FMP100JR-52-3K3	4	\$0.14	\$0.56
Metal Film 100 kΩ 1/4W Res.	DigiKey	1622796-1	4	\$0.41	\$1.64
Metal Film 1.0MΩ	DigiKey	RNF14FTD1M00	8	\$0.15	\$1.20
Trim Pot 100 kΩ	DigiKey	EVN-DJAA03B15	4	\$0.86	\$3.44
Ceramic 0.1 μF Cap.	DigiKey	FK28X7R1H104K	4	\$0.29	\$1.16
Ceramic 1.0 μF Cap.	DigiKey	FK28X5R0J105K	4	\$0.29	\$1.16
Ceramic 10 μF Cap.	DigiKey	FK18X5R0J106M	4	\$0.48	\$1.92
1MFD 50V 0.1μF Cap.	ECE Store	P5179-ND	8	\$0.10	\$0.80
Pin Strip Header	ECE Store	78511-236	1	\$0.82	\$0.82
8-Pin Solder Socket	ECE Store	ED90048-ND	4	\$0.44	\$1.76
4.5"×6.5" Perf Board	ECE Store	64P44	1	\$6.97	\$6.97
				TOTAL	**\$29.51**

D Matlab Code

D.1 Audio Output

```
clear all

samples = 1e4;
Fs = samples; % Number of samples for output
scale = 15; % Increasing scale increases duration of output for 'sweep'
reps = 1; % Number of times the sweep will be performed

% Mode option: 'sweep', 'single'
mode = 'sweep';

switch mode
%% Frequency sweep
    case 'sweep'
        fmin = 10;
        fmax = 200;

        f = fmax:-(fmax-fmin)/(scale*samples):fmin;

        for n = 1:scale*samples
            Y(n) = sin(2*pi*f(n)*n/samples);
        end

        Z = Y;

        for n = 1:reps
            if n == 1
            else
            Z = [Z Y];
            end
        end
%% Single frequency
    case 'single'
        f = 14; % Frequency of tone
        duration = 15; % Duration of tone in seconds

        for n = 1:samples
            Y(n) = sin(2*pi*f*n/samples);
        end

        Z = Y;
        for n = 1:duration
            Z = [Z Y];
        end
end
%% Produce audio output
player = audioplayer(Z, Fs);
play(player)
```

D.2 Read Data from NI myDAQ

```
%% Create myDAQ session and add analog input channels

s = daq.createSession('ni');

In1 = s.addAnalogInputChannel('myDAQ1', 'ai0', 'Voltage');
In2 = s.addAnalogInputChannel('myDAQ1', 'ai1', 'Voltage');

%% Set parameters for the data read

% Sampling rate
s.Rate = 2e3;

% Read duration (1001 for 1-1k; 101 for 1-100)
s.DurationInSeconds = 101;

%% Read in data
clear data timestamps triggerTime

[data, timestamps, triggerTime] = s.startForeground;
```

D.3 Gain Calculations

```
%% Clear
clear all

%% Load preamp magnitude response data
% Files paths removed for brevity

size1 = size(preamp1);

%% Adjust for DC offset
preamp1(1:end,1) = preamp1(1:end,1) - mean(preamp1(1:end,1));
preamp2(1:end,1) = preamp2(1:end,1) - mean(preamp2(1:end,1));
preamp3(1:end,1) = preamp3(1:end,1) - mean(preamp3(1:end,1));
preamp4(1:end,1) = preamp4(1:end,1) - mean(preamp4(1:end,1));

adj_data = [preamp1 preamp2 preamp3 preamp4];

%% Calculate RMS gains
rmssize = 1000; % Set equal to step interval in sweep

rms = zeros(size1(1)-rmssize,8);

for m = 1:2:7
    for n = 1:(size1(1)-rmssize)
        rms(n,m) = sqrt(mean((adj_data(n:n+rmssize,m)).^2));
        rms(n,m+1) = sqrt(mean((adj_data(n:n+rmssize,m+1)).^2));
    end
end

gain1 = rms(1:end,1)./rms(1:end,2);
gain2 = rms(1:end,3)./rms(1:end,4);
gain3 = rms(1:end,5)./rms(1:end,6);
gain4 = rms(1:end,7)./rms(1:end,8);

%% Plots
fstart = 0;
rate = 2000;
f = fstart:100:floor((size1(1)-rmssize)/rate);

% Set ticks for plot
ticks = rate*f;

% Set x axis
x = 1:(size1(1)-rmssize);

for n = 1:size1(1)-rmssize
    simulation(n) = 11;
end

figure(1)
plot(x,simulation,'k--',x,gain1,x,gain2,x,gain3,x,gain4,'linewidth',2)
xlim([0 size1(1)]);
ylim([10.8 11.2])
set(gca, 'XTick',ticks);
set(gca, 'XTickLabel', f);
xlabel('Frequency [Hz]');
ylabel('Gain [V/V]');
grid on
title('Preamplifier RMS Gains')
legend('Simulation','Preamp #1','Preamp #2','Preamp #3','Preamp #4');
```

E Requirements and Verifications Table

Module 1: Microphones

Requirement	Verification	Passed/Failed	Explanation
Microphones have a nominal sensitivity of -50 dB (±3 dB at 94 dB SPL (relative to V_{out} at 74 dB SPL)	Measure voltage outputs at: 0.1 Pa (75 dB SPL) and 1.0 Pa (94 dB SPL)	Passed	-

Module 2: Microphone Probe Housing

Requirement	Verification	Passed/Failed	Explanation
Probe body acoustic interference is minimal (local differences in pressure field simulation with and without microphone do not exceed $10\% \pm 5\%$).	Import CAD files of probe body into COMSOL. Run two simulations for pressure incident on probe and flat surface. Extract pressure at 200 equally spaced points and analyze in MATLAB.	Inconclusive - Test not performed	Simulations could not be preformed reliably in COMSOL. Results were not reproducible and did not pass basic sanity checks (strange local pressures, available acoustic sources simulation methods not physical)
The probe body should be stable against vibrations induced by incident sound waves (lowest eigenfrequeny at no less than 500 Hz ± 100 Hz).	Import CAD files of probe body into COMSOL. Run eigenfrequency simulation and export results.	Inconclusive - Test not preformed.	Simulations could not be preformed reliably in COMSOL. Lowest eigenmode found corresponded to a wavelength much greater than L/2 (lowest expected mode for simple beam of length L).

Module 3: Preamplifiers

Requirement	Verification	Passed/Failed	Explanation
Voltage across microphone power supply terminals must be between 1.0 V and 2.5 V.	Measure voltage across a resistor with resistance equivalent to the microphone (22 kΩ) before installation of microphone. If within range, repeat with microphone.	Passed	-
Mean gain of preamplifier circuit should be 11 V/V with a tolerance of 3%	Simultaneously measure input and output of each preamp and calculate gain. (See verifications section for more detail)	Passed	-
Phase response follows model and is well-characterized at low frequencies	Use an oscilloscope to calculate relative phase between input and output signals	Passed	-

Module 4: Loudspeaker

Requirement	Verification	Pass/Fail	Explanation
Loudspeaker lower-frequency limit characterized	Connect microphone and preamplifier to oscilloscope and play pure sinusoidal tones through the loudspeaker. Use the oscilloscope's frequency-detection functionality to determine lower limit of performance	Completed	-

References

[1] J. Borth, "Survey of Free-Field Methods to Measure the Normal Specific Acoustic Impedance of Ground Surfaces In-Situ at Low Frequencies," M.S. Thesis, Dept of Elect. and Comput. Eng., Univ. of Illinois, Urbana-Champaign, 2013.

[2] F. Fahy, *Sound Intensity,* 1st ed. New York, NY: Elsevier Applied Science, 1989.

[3] L. Kinsler, et al., *Fundamentals of Acoustics*, 4th ed. Hoboken, NJ: Wiley, 2000.

[4] S. Errede, "Lecture XIII: Measurement of Complex Sound Fields, Various Types of Pressure and Particle Velocity Microphones," class notes for PHYS 406, Department of Physics, University of Illinois at Urbana-Champaign, Apr. 3, 2013.